



Università degli Studi Mediterranea di Reggio Calabria
Archivio Istituzionale dei prodotti della ricerca

Engineering seismic demand in the 2012 Emilia sequence: preliminary analysis and model compatibility assessment

This is the peer reviewed version of the following article:

Original

Engineering seismic demand in the 2012 Emilia sequence: preliminary analysis and model compatibility assessment / Iervolino, L., De Luca, F., Chioccarelli, E.. - In: ANNALS OF GEOPHYSICS. - ISSN 2037-416X. - 55:4(2012), pp. 639-645. [10.4401/ag-6118]

Availability:

This version is available at: <https://hdl.handle.net/20.500.12318/62796> since: 2021-01-13T11:16:56Z

Published

DOI: <http://doi.org/10.4401/ag-6118>

The final published version is available online at: <https://www.annalsofgeophysics.eu/index>.

Terms of use:

The terms and conditions for the reuse of this version of the manuscript are specified in the publishing policy. For all terms of use and more information see the publisher's website

Publisher copyright

This item was downloaded from IRIS Università Mediterranea di Reggio Calabria (<https://iris.unirc.it/>) When citing, please refer to the published version.

(Article begins on next page)

Engineering seismic demand in the 2012 Emilia sequence: preliminary analysis and model compatibility assessment.

Iunio Iervolino, Flavia De Luca, and Eugenio Chioccarelli.

Subject classification: Ground motion, Seismic risk.

1. Introduction

The 2012 Emilia sequence featured seven events of moment magnitude (M) larger than 5, five of them occurred between May 20th and May 29th. Earthquakes were structurally damaging over a wide area. Damages include partial or total collapse of industrial precast reinforced-concrete (RC) structures, historical masonry, and mainly non-structural damages to RC buildings; see Section 8 for a damage reports' repository. These structural typologies are, in principle, sensitive to different ground motion (GM) intensity measures (IMs). For example, loss of support requires significant displacement demand at relatively long periods, while infilling damages are due to GM amplitude at higher frequencies, and masonry structures are comparatively more sensitive to cyclic content of ground shaking. Moreover, because events were concentrated in space and time, it could be argued that the cumulative effect of the sequence contributed to damage.

Because the current seismic code (CS.LL.PP., 2008) uses a seismic hazard map (Stucchi et al., 2011) to determine seismic actions for structural design, when a strong earthquake occurs probabilistic estimates are understandably questioned for consistency with respect to observed GM. While it is easy to prove (e.g., Iervolino, 2012) that hazard, in terms of frequency of occurrence of IM, can be hardly validated via the records of a single earthquake; on the other hand, it can be certainly verified whether the observations are compatible or atypical with respect to what predicted by the tools employed in best practice hazard studies.

These issues mostly motivated the preliminary analysis briefly presented in this letter, that is, to investigate engineering seismic demand (peak and cyclic) and to compare it with prediction models. Both elastic and inelastic demands were considered. In fact, the latter is more important from the structural engineering point of view.

Considered waveforms refer to the M 6 May 20th and the M 5.9 May 29th events; i.e., those made available by the national accelerometric network (RAN – *Rete Accelerometrica Nazionale*); see Data and Sharing Resources Section.

Although several recordings, up to hundreds of kilometers far from the sources, are available,

most of this study focuses on five seismic stations, within 50 km from the epicenters of both earthquakes (within R1 and R2 in Figure 1).

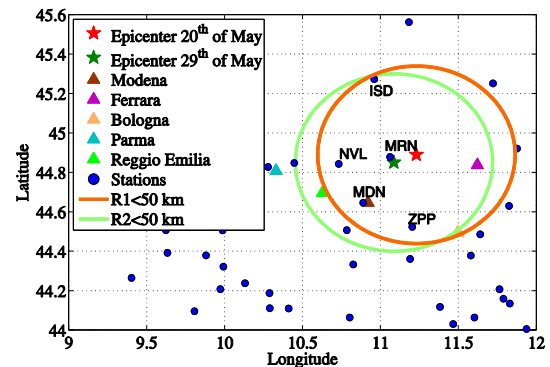


Figure 1. RAN recording stations within about 200 km from the epicenters, and those considered within 50 km.

This letter is structured such that, peak and integral GM-IMs are provided first for the five close stations. Subsequently, the comparison with several ground motion prediction equations, or GMPEs, is given for all RAN stations up to 650 km from the epicenters. For those stations closer to the source, recorded elastic pseudo-acceleration response spectra (S_a) are also superimposed to the predictions according to Bindi et al. (2011) GMPE, and to design spectra for 475 and 2475 yr return periods (T_r). The inelastic displacement spectra for selected structural systems are given and discussed with respect to recently developed semi-empirical models (i.e., De Luca, 2011; De Luca et al., 2012). The same is carried out with respect to the *equivalent number of cycles* (N_e), a measure of how GM damaging potential is distributed over the entire waveform (Iervolino et al., 2006). Finally, kinematic ductility (μ) is analyzed to understand whether the sequence was ordinary with respect to engineering demand. Close records were also checked for forward directivity effects. The study, finally, includes consideration of the *cumulative inelastic demands* from the two events, to measure the effects of repeated shocks on structures. In fact, what presented in the following is based on the more extended reports by Chioccarelli et al. (2012a and 2012b), where further analyses and discussions can be found.

2. Processing and assumptions

At the time of the study, limited information was available to the authors with respect to source

geometries. Therefore, in all the cases in which the closest distance to the fault plane projection (R_{jb}) was necessary, an empirically calibrated model (Montaldo et al., 2005) was used, neglecting uncertainty, to convert epicentral distance (R_{epi}). Moreover, because only a linear baseline was originally applied to waveforms by the data provider, records were further processed applying a fourth-order bandpass Butterworth filter with a frequency range of 0.25-25 Hz. Such a procedure does not differ significantly with respect to that employed for the Italian ACcelerometric Archive or ITACA (e.g., Pacor et al., 2011).

3. Peak and cyclic intensity measures

In this section, IMs of considered records are analyzed. First, peak ground acceleration (PGA), peak ground velocity (PGV) and Sa, are compared to Bindi et al. (2011) GMPE, for both May 20th (Figure 2) and May 29th (Figure 3) events. GMPE plots refer to A-type site class according to

CS.LL.PP. (2008), as soil classification was not available to the authors, for all stations. Even with this approximation, a general agreement is found between data and prediction models. Comparisons are reported for geometric mean of horizontal and for vertical components of ground motion. For the sake of brevity, only PGA, PGV and two Sa ordinates at period (T) equal to 0.3s and 1.0s are shown. GMPE predictions are represented by median values and median plus or minus one total standard deviation ($Median + \sigma$ and $Median - \sigma$, respectively). The interested reader may find these and other comparisons, also in terms of GMPEs residuals, in Chioccarelli et al. (2012a and 2012b). Arias intensity (I_A) was also considered. I_A , the largest among the horizontal components of each record divided by $\pi/(2 \cdot g)$, is compared to the Sabetta and Pugliese (1996) GMPE (Figure 4). In this case the agreement appears of a lower grade; however, several data-points fall outside the applicability range of the GMPE.

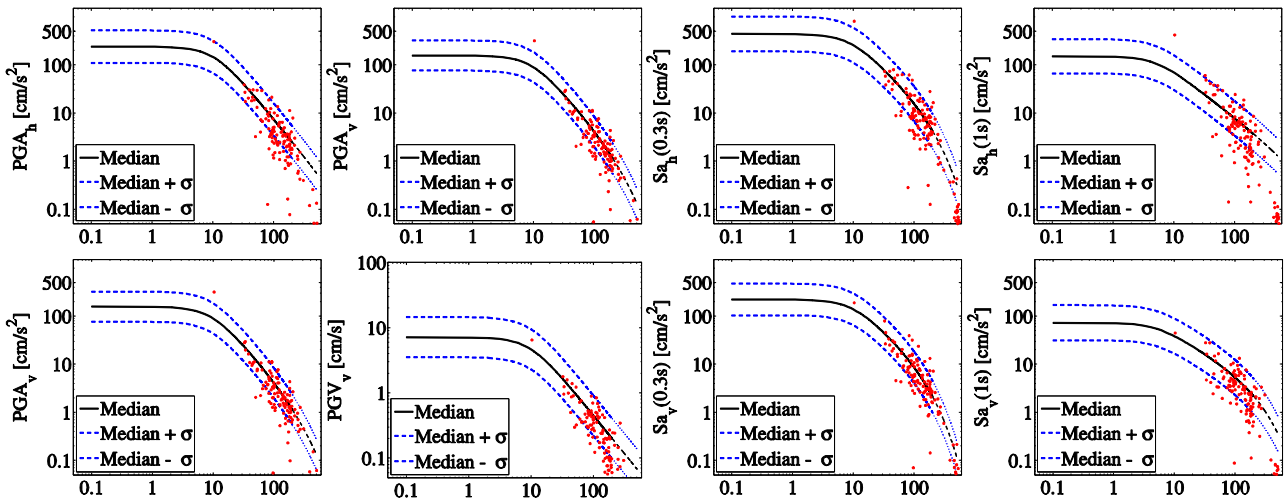


Figure 2. May 20th event: comparison with GMPE in terms of PGA, PGV, Sa(0.3s), Sa(1.0s) for the geometric mean of the horizontal (h-subscript) and for the vertical (v-subscript) components of GM. Horizontal axis is always R_{gm} [km].

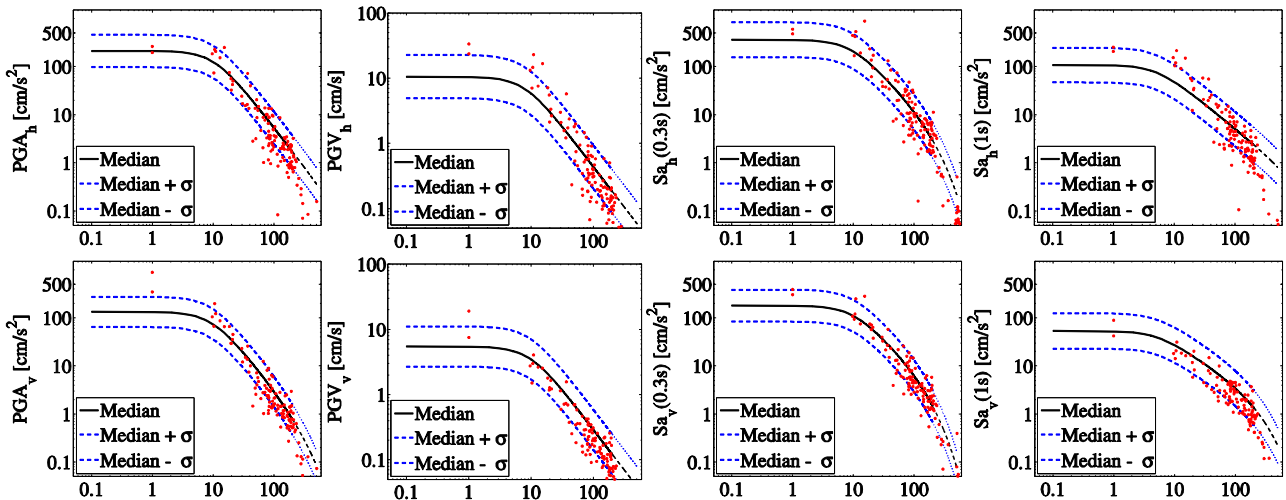


Figure 3. May 29th event: comparison with GMPE in terms of PGA, PGV, Sa(0.3s), Sa(1.0s) for the geometric mean of the horizontal (h-subscript) and for the vertical (v-subscript) components of GM. Horizontal axis is always R_{gm} [km].

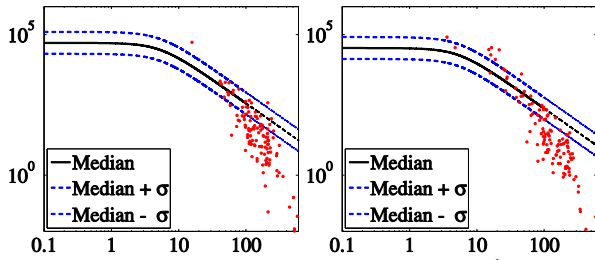


Figure 4. I_A data versus GMPE, for the May 20th (left) and the May 29th (right) events. Horizontal axis is always R_{epi} [km]. Vertical axes are I_A divided by $\pi/(2 \cdot g)$ [cm^2/s^3].

Table 1 summarizes peak and integral parameters of GM for all components of the five records within 50 km from the epicenters. More specifically, for both events, reported IMs are: PGA, PGV, I_A , Cosenza and Manfredi Index (I_D , a measure of the cyclic damage potential of ground motion; Iervolino et al., 2006), and Housner Intensity (H_{50}).

Local site conditions (S) were obtained from ITACA, except ZPP station, for which S was not available. An A-type site class was then assumed for ZPP.

The five percent damped elastic pseudo-acceleration response spectra are compared in Figure 5 with median spectra corresponding to M , R_{jb} and site class (plus and minus one standard deviation) from the Bindi et al. (2011) GMPE. The comparison indicates that elastic demand in all GM components does not appear atypical.

4. Discussion with respect to design spectra

In Figure 6 the spectra for MRN station (the closer to both epicenters) is compared to design spectra, for A- and D-type soil classes (as amplitude bounds) from the Italian code (CS.LL.PP., 2008). Those referring to A-type site class basically are uniform hazard spectra (UHS) for 475 yr and 2475 yr Tr (an arbitrary, yet wide, range) from probabilistic hazard; i.e., Stucchi et al., 2011. At MRN station, the recorded spectra

are comparable or larger than the high Tr UHS. This may be interpreted as if the probabilistic hazard is underestimating the hazard in the area. However, the same figure clearly shows that the other nearby stations experienced response spectra generally much below the design spectra. In fact, when probabilistic hazard is compared to observed ground motion, the latter is always taken at the maximum value, that is, as close as possible to the source of the earthquake. This is obvious and perfectly understandable. However, when arguing about possible underestimations of probabilistic seismic hazard studies, one should consider that these average (via the total probability theorem) all possible epicentral locations. In fact, the probabilistic hazard, computed assuming that the epicenter is the site of interest, would be certainly larger than the case the epicentral location is spread on all possible locations within the source. Because in an earthquake, a specific (yet uncertain) site will be the epicenter, comparing the recorded spectrum with probabilistic hazard spectrum, for that site only, can be misleading, and a verification should be carried out also considering other non-epicentral stations (e.g., Albarello and D'Amico, 2008; McGuire and Barnhard, 1981). This check for the Emilia events confirms that it is not possible to question the probabilistic hazard solely on the basis of the spectrum at the epicenter. (This is also because intrinsic limits, especially in the near-source region, of GMPEs and of the UHS, which cannot be addressed herein for the sake of brevity.) On the other hand, to check whether actual magnitude and source features were appropriately accounted for in the models considered to carry out hazard, as well as suitability of GMPEs used in the analysis (i.e., other comparisons herein), could be more appropriate verifications (Iervolino (2012).

Table 1. Peak and integral IMs of the five stations within an epicentral distance smaller than 50 km. E-W is east-west, N-S is north-south, referring to horizontal components. V refers to the vertical component.

Station IDs	Comp.	S	R_{epi} [km]		PGA [cm/s^2]		PGV [cm/s]		I_A [cm/s]		I_D		H_{50} [cm]	
			20 th	29 th	20 th	29 th	20 th	29 th	20 th	29 th	20 th	29 th	20 th	29 th
Mirandola (MRN)	N-S	C	16	4	313	267	45	54	86.8	132.6	3.8	5.7	127.5	134.8
	E-W				295	256	23	21	71.4	78.9	6.4	9.3	82.4	67.7
	V				317	883	6	19	43.6	289.9	13.2	10.8	16.0	25.7
Modena (MDN)	N-S	C	41	28	38	54	4	4	2.7	4.4	10.4	12.8	12.4	14.9
	E-W				39	33	4	3	3.5	2.8	13.0	19.1	14.0	10.4
	V				28	35	2	2	1.3	1.8	16.4	19.1	5.4	6.5
Novellara (NVL)	N-S	C	42	28	48	45	2	3	2.6	4.8	15.6	25.2	7.1	10.1
	E-W				48	55	3	3	2.8	5.0	13.1	21.6	7.5	10.5
	V				29	45	1	1	0.9	2.6	20.5	29.7	1.6	2.3
Zola Pedrosa Piana (ZPP)	N-S	A	43	38	21	24	4	3	2.7	2.1	18.9	16.7	15.5	12.7
	E-W				15	24	2	3	1.5	1.8	27.5	16.9	9.0	9.4
	V				20	23	1	1	0.8	0.7	21.0	15.6	4.6	3.3
Isola Della Scala (ISD)	N-S	B	47	48	16	15	2	2	0.9	1.1	22.4	20.4	7.0	8.3
	E-W				15	12	2	1	0.9	0.5	23.5	19.0	7.6	4.8
	V				9	7	1	1	0.2	0.2	17.3	21.5	2.5	2.3

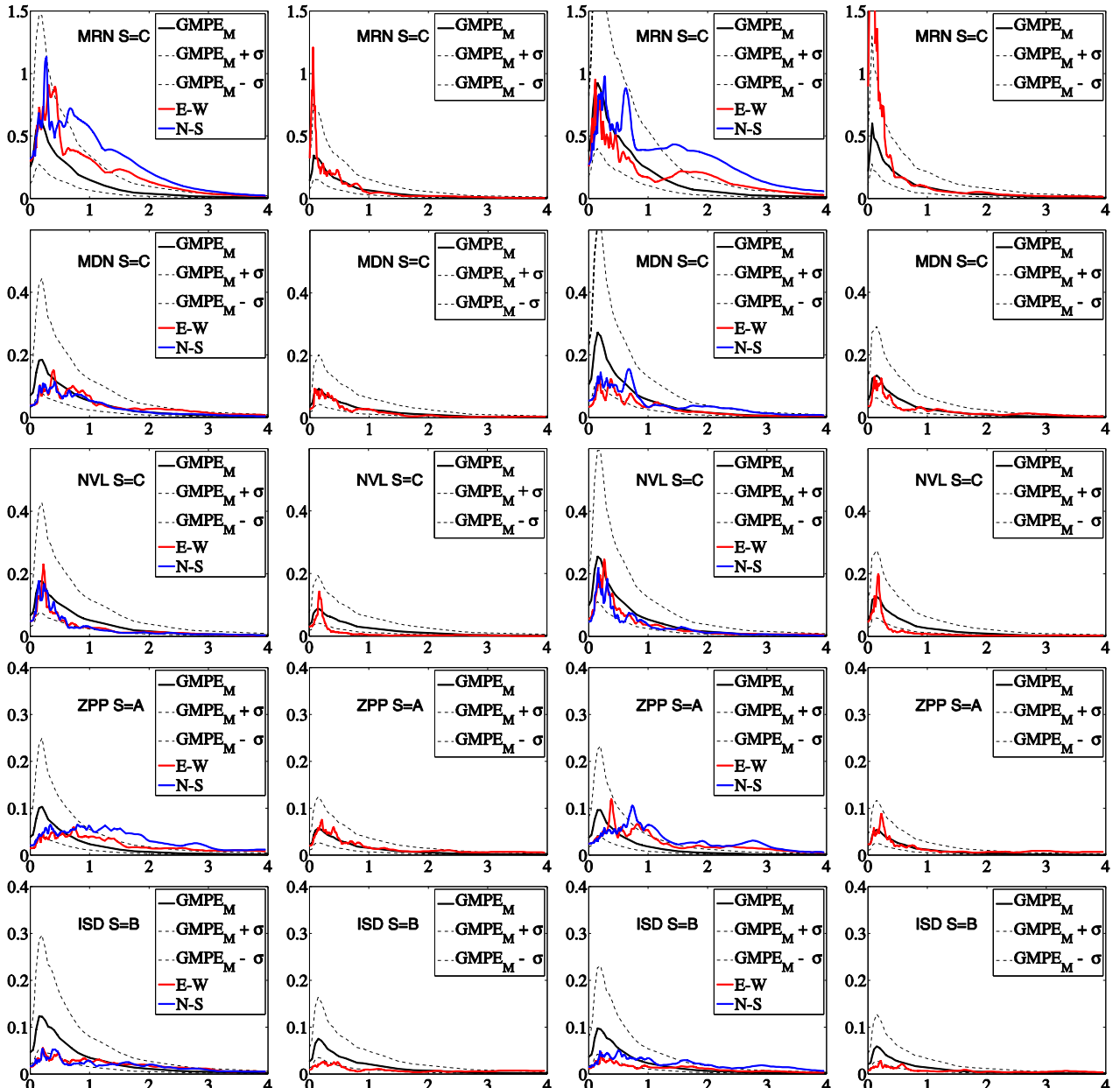


Figure 5. Comparison between GMPE-predicted and actual spectra for the May 20th (first and second columns from the left) and the May 29th (third and fourth columns from the left) events. First and third columns refer to horizontal components, while second and fourth column refer to vertical components. The vertical axis is always S_a [g], the horizontal axis is T [s].

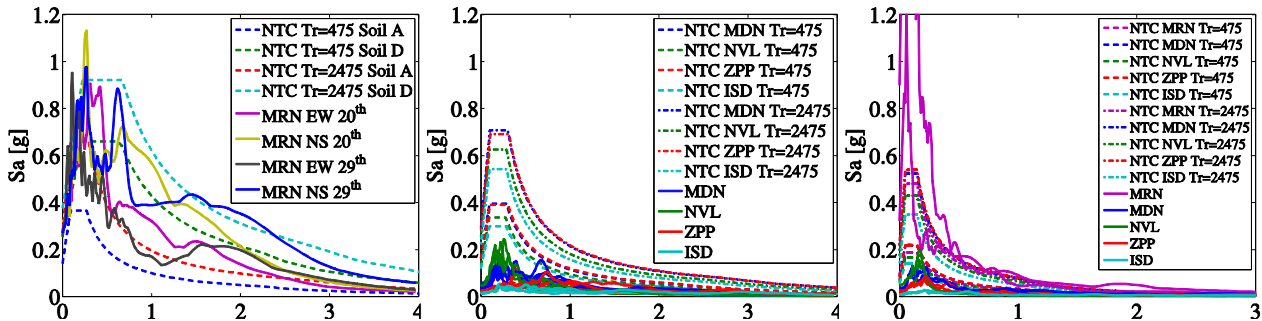


Figure 6. Comparison with code spectra for horizontal components of: MRN station (left), of the other four stations (center), and for the vertical components of all stations (right). The horizontal axis is T [s]. (Vertical component of MRN may be affected by instrumental errors; see Mirandola Earthquake Working Group, 2012.)

5. Inelastic engineering demand

For the five close stations, inelastic peak and cyclic engineering demand parameters (EDPs)

were computed because they are especially relevant to measure earthquake's damage potential. To this aim, two different single degree of freedom (SDoF) systems were selected to

represent generic nonlinear structures: (a) an elastic-plastic backbone with a non-degrading strain hardening hysteretic loop (EPP-k); and (b) an elastic-hardening backbone with a hardening stiffness equal to five percent of that elastic, and a pinching hysteresis rule (EPH-k), Figure 7.

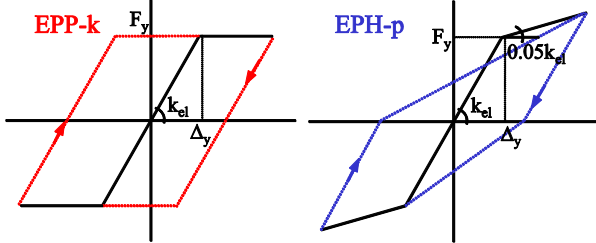


Figure 7. EPH-p and EPP-k SDOFs' constitutive relationships.

For the EPH-p SDOF, EDPs prediction equations were recently developed in terms of constant strength reduction factor (R_μ) GMPEs (i.e., De Luca, 2011; De Luca et al., 2012). R_μ approach is defined in Equation 1, where F_y is the yield strength, and m is the mass of the SDOF.

$$R_\mu = \frac{Sa(T) \cdot m}{F_y} \quad (1)$$

The peak-EDP is the inelastic displacement ($Sd_{R_\mu=i}$) and equivalent number of cycles ($N_{e,R_\mu=i}$).

In Equation 2 the inelastic EDP related to cyclic GM potential is defined, that is, the equivalent number of cycles. N_e is given by the cumulative hysteretic energy (E_H), computed as the sum of the areas of the hysteretic cycles (not considering contribution of viscous damping), normalized with respect to the largest cycle; the latter is the area underneath the monotonic backbone curve from the yielding displacement to the peak inelastic displacement ($A_{plastic}$).

$$N_e = \frac{E_H}{A_{plastic}} + 1 \quad (2)$$

In Figure 8, the nonlinear EDP spectra are compared to the corresponding GMPEs predictions for EPH-p at R_μ equal to 6. As a benchmark, also elastic spectral displacements, Sd_{el} , were computed and compared with the GMPE by De Luca (2011). The comparisons were carried out separately for the two events considered. In addition, the cumulative effect of the sequence was computed ($20^{th}+29^{th}$). Similarly to the elastic comparisons above, results show general agreement of recordings with predictions (except MRN in a selected period range, and ZPP also likely due to the assumed soil conditions).

The peak displacement does not increase significantly for the structure subjected to the series of the two events. Conversely, N_e is

affected by the cumulative effect, which often exceeds the predictions. This means that the series had, as expected, an increased damaging potential for structures sensitive to cyclic demand of GM, with respect to the two events alone.

Referring to the EPP-k backbone of Figure 7, the demand of kinematic ductility (Iervolino et al., 2006) was also computed for horizontal records of the five stations within 50 km. The considered SDOF has a fundamental period equal to 0.5 s and an R_μ factor equal to 6 for the design spectral acceleration at the MRN station, for D-type site class and T_r equal to 475 yr, that is, 0.66g. Results are summarized in Table 2 for MRN only, because response computed for the other stations did not produce any inelastic behavior, that is, ductility demand was always zero for that specific system (consistent with Figure 6, which indicates somewhat weak motion for them). On the other hand, ductility demand at MRN was significant for both events.

Table 2. Kinematic ductility demand for MRN station.

Station and component		μ_1 (May 20 th)	μ_2 (May 29 th)	$\mu_1 + \mu_2$
MRN	E-W	5.3	3.7	8.9
MRN	N-S	10.4	13.8	24.2

6. Forward directivity check

Recorded GMs of the stations within 50 km from the epicenters were investigated with respect to possible directivity effects. The records were searched for predominant pulses in the velocity time-history (e.g., Chioccarelli and Iervolino, 2010). Given that the rupture was unknown, for each station time-histories were rotated in all the possible horizontal directions and analyzed. No evidence of significant forward directivity effect of structural relevance was found; (see Chioccarelli et al. (2012a and 2012b) for details.

7. Conclusions

A preliminary analysis of the records of the two strongest events in the 2012 Emilia sequence was presented. The analyses were carried out to infer whether engineering seismic demand might be considered ordinary; i.e., somewhat expected for events of this kind. This was done mainly for the stations closer to the source, comparing recorded response with recent prediction models based on Italian datasets. Analyses were carried out in terms of: (1) peak and cyclic ground motion intensity measures; (2) elastic spectral ordinates; (3) inelastic peak and cyclic structural demands. In the latter case, effects of the seismic sequence were also considered.

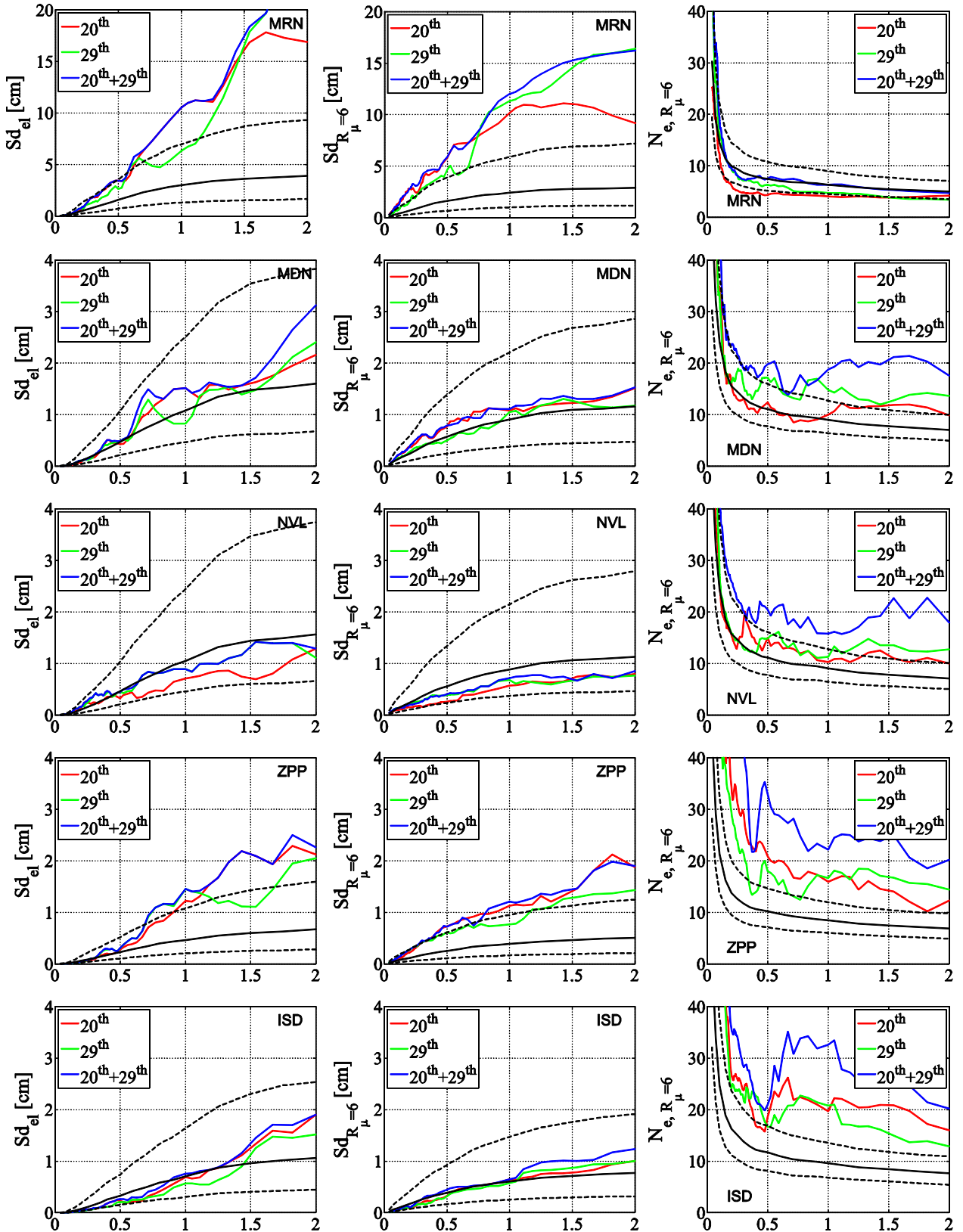


Figure 8. May 20th event: geometric mean of horizontal elastic and inelastic displacements (first two columns), and equivalent number of cycles spectra (third column) evaluated separately for the two events (20th and 29th) and for the sequence (20th + 29th), compared with GMPEs by De Luca (2011) and De Luca et al. (2012). Horizontal axis is always T [s].

Results indicate that, generally, recorded ground motions cannot be considered atypical, in terms of elastic and inelastic, and peak and cyclic, demands. It was also found that, as expected, the

seismic series had a significant cyclic and ductility damage potential, when compared to the two events individually. This is especially meaningful considering that the short interevent

time did not allow for repair of several damaged structures after the first earthquake.

The comparison with design spectra show that ground motion is comparable with high return period predictions only at the epicenter. It was briefly discussed why this is not a sufficient argument to question probabilistic hazard studies.

Finally, the records were searched for near-source forward directivity effects. The velocity time-histories, apparently, do not show any full velocity cycle of structural engineering interest.

8. Data and Sharing Resources

Records used in this study were made available by the Italian Civil Protection Department (*Dipartimento della Protezione Civile Nazionale*, in Italian); the interested reader should refer, for details, to Mirandola Earthquake Working Group (2012) at <http://www.protezionecivile.gov.it>. Soil conditions for some of the recording stations were retrieved from the Italian ACcelerometric Archive (<http://itaca.mi.ingv.it/>). Damage reports for the Emilia sequence are available at <http://www.reluis.it/>.

Acknowledgments

This work was carried out in the ReLUIIS 2010-2013 research program founded by *Dipartimento della Protezione Civile*. The two anonymous reviewers, whose comments improved quality and readability of the paper, are gratefully acknowledged.

References

- Albarelo, D., V. D'Amico (2008) Testing probabilistic seismic hazard estimates by comparison with observations: an example in Italy, *Geophys. J. Int.*, 175, 1088–1094.
- Bindi, D, F. Pacor, L. Luzi, R. Puglia,, M. Massa, G. Ameri, R. Paolucci (2011). Ground motion prediction equations derived from the Italian strong motion database. *Bulletin of Earthquake Engineering*, 9, 1899-1920.
- Chioccarelli, E, Iervolino, I. (2010) Near-source seismic demand and pulse-like records: a discussion for L'Aquila earthquake. *Earthq. Engn. Struct. Dyn.*, 39, 1039–1062.
- Chioccarelli, E., F. De Luca and I. Iervolino (2012a). Preliminary study of Emilia (May 20h 2012) earthquake ground motion records V2.11. (Available at <http://www.reluis.it>)
- Chioccarelli, E., F. De Luca and I. Iervolino (2012b). Preliminary study of Emilia (May 29th 2012) earthquake ground motion records V1.0. Available at <http://www.reluis.it>)
- CS.LL.PP; DM 14 Gennaio (2008). Norme tecniche per le costruzioni, 2008. *Gazzetta Ufficiale della Repubblica Italiana*, 29 (In Italian).
- De Luca, F, G. Ameri, I. Iervolino, F. Pacor and D. Bindi (2012). Prediction equations for peak and cyclic engineering seismic response based on Italian data. *Earthquake Spectra*. (Under review).
- De Luca, F. (2011). Records, capacity curve fits and reinforced concrete damage states within a performance based earthquake engineering framework. PhD thesis.

Department of Structural Engineering, University of Naples Federico II. Advisors: G. Manfredi, I. Iervolino, G.M. Verderame. (Aavailable at <http://wpage.unina.it/iuniervo/>)

- Iervolino, I. (2012). Probabilità e salti mortali: le insidie della validazione dell'analisi di pericolosità attraverso l'occorrenza di singoli terremoti. *Progettazione Sismica*, 3. IUSS Press, Pavia, Italy. (in Italian, in press)
- Iervolino, I., G. Manfredi and E. Cosenza (2006). Ground motion duration effects on nonlinear seismic response. *Earthq. Engn. Struct. Dyn.*, 35, 21–38.
- McGuire, R.K., T.P. Barnhard, (1981). Effects of temporal variations in seismicity on seismic hazard, *Bull. seism. Soc. Am.*, 71, 321–334.
- Mirandola Earthquake Working Group (2012), Reports 1,2.
- Montaldo, V., E. Faccioli, G. Zonno, A. Akinci and L. Malagnini (2005). Treatment of ground-motion predictive relationships for the reference seismic hazard map of Italy. *Journal of Seismology*, 9, 295–316.
- Pacor, F., R. Paolucci, G. Ameri, M. Massa and R. Puglia, (2011). Italian strong motion records in ITACA: overview and record processing. *Bull. Earthq. Engn.*, 9, 1741-1759.
- Sabetta, F. and A. Pugliese (1996). Estimation of Response Spectra and Simulation of Nonstationary Earthquake Ground Motion. *Bull. Seism. Soc. Am.*, 86, 337-352.
- Stucchi, M., C. Meletti, V. Montaldo, H. Crowley, G.M. Calvi and E. Boschi (2011). Seismic Hazard Assessment (2003-2009) for the Italian Building Code. *Bull. Seism. Soc. Am.*, 101, 1885-1911.

Corresponding author: Iunio Iervolino, Dipartimento di Ingegneria Strutturale, Università degli Studi di Napoli Federico II, Via Claudio 21, 80125 Naples – Italy;
Tel: +39 081 7683488, Fax: +39 081 7683491;
email: iunio.iervolino@unina.it